Scissors resonance in the quasicontinuum of Th, Pa, and U isotopes

M. Guttormsen,[1,*] L. A. Bernstein,[2] A. Görgen,[1] B. Jurado,[3] S. Siem,[1] M. Aiche,[3] Q. Ducasse,[3] F. Giacoppo,[1] F. Gunsing,[4] T. W. Hagen,[1] A. C. Larsen,[1] M. Lebois,[5] B. Leniau,[5] T. Renstrøm,[1] S. J. Rose,[1] T. G. Tornyi,[1,6] G. M. Tveten,[1] M. Wiedeking,[7] and J. N. Wilson[5]

[1]*Department of Physics, University of Oslo, N-0316 Oslo, Norway*
[2]*Lawrence Livermore National Laboratory, 7000 East Avenue, Livermore, California 94550-9234, USA*
[3]*CENBG, CNRS/IN2P3, Universit Bordeaux, Chemin du Solarium B.P. 120, 33175 Gradignan, France*
[4]*CEA Saclay, DSM/Irfu/SPhN, F-91191 Gif-sur-Yvette Cedex, France*
[5]*Institut de Physique Nucleaire d'Orsay, Bâtiment 100, 15 rue G. Glemenceau, 91406 Orsay Cedex, France*
[6]*Institute of Nuclear Research of the Hungarian Academy of Sciences (MTA Atomki), Debrecen, Hungary*
[7]*iThemba LABS, P.O. Box 722, 7129 Somerset West, South Africa*

(Received 25 October 2013; published 6 January 2014)

The γ-ray strength function in the quasicontinuum has been measured for $^{231–233}$Th, ^{232,233}Pa, and $^{237–239}$U using the Oslo method. All eight nuclei show a pronounced increase in γ strength at $\omega_{SR} \approx 2.4$ MeV, which is interpreted as the low-energy $M1$ scissors resonance (SR). The total strength is found to be $B_{SR} = 9–11\ \mu_N^2$ when integrated over the 1–4 MeV γ-energy region. The SR displays a double-hump structure that is theoretically not understood. Our results are compared with data from (γ, γ') experiments and theoretical sum-rule estimates for a nuclear rigid-body moment of inertia.

DOI: 10.1103/PhysRevC.89.014302 PACS number(s): 23.20.−g, 24.30.Gd, 27.90.+b

I. INTRODUCTION

Atomic nuclei in the actinide region are unique from an astrophysics point of view, because they are purely made in rapid neutron-capture processes in explosive stellar environments [1]. Attempts have been made to use the abundances of ^{232}Th and ^{235,238}U observed in the solar system (measured from meteoritic analyses) to estimate the age of the Galaxy, although these estimates are very uncertain and model-dependent. Thorium has been observed in stars similar to the Sun, and also in older metal-poor stars [1].

To predict the abundance of the actinides, one has to know the relevant reaction rates not only for the most long-lived nuclei, e.g., ^{232}Th (14.05 Gy) and ^{238}U (4.468 Gy), but also for the ones with extremely high neutron excess. Therefore, one must rely on calculations to estimate unknown cross sections where experimental data are lacking. This is not only relevant for the astrophysical nucleosynthesis [1,2], but also for future and existing nuclear reactors [3].

Together with optical-model potentials, the nuclear level density and γ-ray strength function (γSF) are crucial inputs for calculating neutron-induced reaction cross sections for neutron energies above the neutron-resonance region. These quantities provide information on the average properties of excited nuclei and are particularly applicable for describing gross features in the quasicontinuum region, where the number of levels is too high to measure individual states and their transitions. To ensure a reliable estimation of unknown cross sections, a detailed knowledge of both the level density and γSF is vital.

An enhancement of the γSF may boost the γ decay relative to other decay branches such as particle emission or fission. For the actinides, which have deformed shapes, the low-energy orbital $M1$ scissors resonance (SR) contributes significantly to the γ-decay probability.

The first geometrical description of the SR was given by Lo Iudice and Palumbo [4]. Naively, the SR can be viewed as the proton and neutron clouds oscillating against each other like scissor blades. For deformed nuclei, Chen and Leander [5] predicted strong $M1$ transitions between $\Delta\Omega = 1$ Nilsson orbitals[1] originating from the same spherical state. These predictions were later supported by the observation of an enhancement at $E_\gamma \approx 2.2$ MeV in the γ spectra of the excited ^{161}Dy nucleus [6].

Discrete scissors states built on the ground state can be populated in the (γ, γ') and (e,e') reactions. Here, the strength, spin, and in some cases the parity of the strongest scissors states in ^{232}Th and ^{235,236,238}U have been determined with typical summed strengths of $B_{SR} \sim 3–4\ \mu_N^2$ [7–10], where μ_N is the nucleon magneton. Because such measurements rely on the identification of single states in an energy region of 10^4–10^5 levels per MeV, it is reasonable to believe that not all the strength has been experimentally resolved.

Recently [11], a review of several experiments and various models on the SR has been presented. The microscopic description of the SR is based on single-particle couplings between orbitals of the same angular momentum ℓ and j. These proton and neutron two-quasiparticle configurations contribute in a more or less coherent way. Therefore, the macroscopic picture of oscillating scissors blades is rather oversimplified. Recent quasiparticle random phase approximation (QRPA) calculations [11,12] are generally in agreement with the

*magne.guttormsen@fys.uio.no

[1]The single-particle Nilsson orbitals are labeled by $\Omega^\pi[Nn_z\Lambda]$, where Ω is the projection of the angular momentum vector j on the nuclear symmetry axis.

 ©2014 American Physical Society

observed energies of the scissors states and strengths observed in (γ, γ') and (e,e') reactions.

According to the generalized Brink hypothesis [13], the SR is not only built on the nuclear ground state, but on all excited states in the nucleus. The Oslo method, which is based on particle-γ coincidences, makes it possible to explore the decay of SR states in the quasicontinuum region. The method permits the extraction of both level density and γSF in one and the same experiment [14,15]. These measurements cover the rather unexplored γ- and excitation-energy region up to the neutron binding energy (or the threshold for fission). Recently, the level densities of $^{231-233}$Th and $^{237-239}$U [16] and the γSFs in $^{231-233}$Th and ^{232,233}Pa [17] using this method have been reported.

The main purpose of the present work is to make a comprehensive and systematic analysis of several actinides by exploiting nine reactions in total. The previous data of the γSFs of $^{231-233}$Th and ^{232,233}Pa [17] are reanalyzed and new experiments on $^{237-239}$U are presented. In addition, the level densities of ^{232,233}Pa are reported for the first time.

The structure of the manuscript is as follows. Section II describes the experimental techniques and methods, and in Sec. III the extraction and normalization of the γSFs are discussed. In Sec. IV the SRs are presented and extracted resonance parameters are given. Section V compares the data with previous results and models. Conclusions are drawn in Sec. VI.

II. EXPERIMENTS

The experiments with were performed with the MC-35 Scanditronix cyclotron at the Oslo Cyclotron Laboratory (OCL). The selfsupporting ^{232}Th target (thickness 0.968 mg/cm^2) was bombarded with a 12-MeV deuteron beam and a 24-MeV ^{3}He beam. The ^{238}U target (thickness 0.260 mg/cm^2 and enrichment 99.7%) had a carbon backing (thickness 0.043 mg/cm^2) and was bombarded with a 15-MeV deuteron beam. Particle-γ coincidences were measured with the SiRi particle telescope and the CACTUS γ-detector system [18,19].

In order to reduce the intense elastically scattered projectiles on the detectors and exposure of deuteron break-up, the 64 SiRi telescopes were placed in backward direction covering eight angles from $\theta = 126^\circ$ to 140° relative to the beam axis. These angles also give a broader and higher spin distribution that are in better agreement with the real spin distribution of the nucleus. The front and back detectors have thicknesses of 130 and 1550 μm, respectively. The CACTUS array consists of 28 collimated $5'' \times 5''$ NaI(Tl) detectors with a total efficiency of 15.2% at $E_\gamma = 1.33$ MeV.

The particle-γ coincidences with time information were sorted event by event. Gates were set on the 64 ΔE-E matrices to select various particle types. From the known charged-particle type and the kinematics of the reaction, the energies deposited in the telescopes can be translated to initial excitation energy E in the residual nucleus. To avoid contamination from γ rays emitted by the fission fragments, we consider only excitation energies below the fission barrier. For each energy bin E, the γ spectra are unfolded [20] using

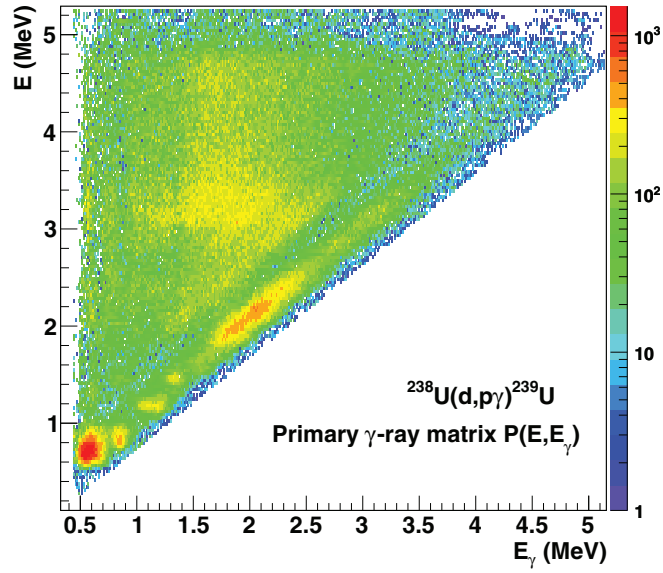

FIG. 1. (Color online) First generation (primary) γ-ray matrix in ^{239}U. At each excitation energy bin, γ spectra can be projected out, giving the energy distribution of the first γ's from that excitation energy. The excitation energy (E) and γ energy (E_γ) axis have dispersion 14.0 keV/ch and 32.4 keV/ch, respectively.

new NaI-response functions based on several in-beam γ lines from excited states in ^{13}C, ^{16,17}O, ^{28}Si, and ^{56,57}Fe, where the relative detector efficiency as function of γ energy could be extracted in a reliable way.

An iterative subtraction technique was applied to separate out the first-generation (primary) γ transitions from the total γ cascade [21]. The technique is based on the assumption that the γ distribution is the same whether the levels were populated directly by the nuclear reaction or by γ decay from higher-lying states. This assumption is necessarily fulfilled when states have the same relative probability to be populated by the two processes, since γ-branching ratios are properties of the levels themselves. If the excitation bins contain many levels, as is the case for the actinides, it is likely to find the same γ distribution independent of the method of population. Figure 1 shows the final first-generation γ-ray matrix $P(E,E_\gamma)$ for the ^{238}U$(d,p\gamma)^{239}$U stripping reaction.

Fermi's golden rule predicts that the decay probability may be factorized into a transition matrix element between the initial and final states, and the density of final states [22,23]. Furthermore, according to the Brink hypothesis [13], the γ-ray transmission coefficient $\mathcal{T}$ is approximately independent of excitation energy. The first-generation matrix $P(E,E_\gamma)$, which expresses the probability to emit a γ-ray with energy E_γ from excitation energy E, may therefore be factorized as follows:

$$P(E,E_\gamma) \propto \mathcal{T}(E_\gamma)\rho(E - E_\gamma), \quad (1)$$

where $\rho(E - E_\gamma)$ is the level density at the excitation energy after the first γ-ray has been emitted in the cascades. This factorization allows a simultaneous extraction of level density and γ-ray transmission coefficient since the number of data points of the $P(E,E_\gamma)$ matrix exceeds by far the number of unknown data points of the vectors $\mathcal{T}(E_\gamma)$ and $\rho(E - E_\gamma)$. The

TABLE I. Parameters used to extract level densities and γSFs (see text).

Reaction and final nucleus	S_n (MeV)	$\sigma(S_n)$	D_0 (eV)	$\rho(S_n)$ (10^6 MeV^{-1})	$\rho(S_n)_{\text{adopted}}$ (10^6 MeV^{-1})	$\langle\Gamma_\gamma(S_n)\rangle$ (meV)	$\langle\Gamma_\gamma(S_n)\rangle_{\text{adopted}}$ (meV)
(^{3}He,α) $^{231}_{90}$Th	5.118	7.78	9.6(15)	12.7(33)	12.7	26(2)	26
(d, d') $^{232}_{90}$Th	6.438	8.05	0.78(20)[a]	30(8)[a]	20	30(10)[a]	40
(^{3}He,^{3}He$'$) $^{232}_{90}$Th	6.438	8.05	0.78(20)[a]	30(8)[a]	30	30(10)[a]	40
(d, p) $^{233}_{90}$Th	4.786	7.81	16.5(4)	7.4(15)	4.0	24(2)	20
(^{3}He, t) $^{232}_{91}$Pa	5.549	8.19	0.51(3)	68(13)	68	40(1)	35
(^{3}He, d) $^{233}_{91}$Pa	6.529	8.82	0.42(8)	77(21)	77	30(10)[a]	45
(d, t) $^{237}_{92}$U	5.126	8.02	14.0(10)	9.3(19)	7.4	23(2)	26
(d, d') $^{238}_{92}$U	6.154	8.26	3.5(8)	20(6)	20	30(10)[a]	55
(d, p) $^{239}_{92}$U	4.806	7.84	20.3(6)	6.1(12)	2.45	23.6(8)	33

[a]Estimated from systematics [25].

least-square fit of $\mathcal{T}\rho$ to P [see Eq. (1)] determines only the functional form of $\mathcal{T}$ and ρ. If one solution of the functions $\mathcal{T}$ and ρ is known, one may construct identical fits to the $P(E,E_\gamma)$ matrix by

$$\tilde{\rho}(E-E_\gamma) = A\exp[\alpha(E-E_\gamma)]\,\rho(E-E_\gamma), \quad (2)$$

$$\tilde{\mathcal{T}}(E_\gamma) = B\exp(\alpha E_\gamma)\mathcal{T}(E_\gamma). \quad (3)$$

The transformation parameters A, α, and B can then be estimated.

The level density function needs two normalization points to deduce A and α of Eqs. (2) and (3). These points are determined at low excitation energy from the known level scheme [24], and at high energy from the density of neutron resonances following (n,γ) capture at the neutron separation energy S_n. Here, the data point $\rho(S_n)$ is calculated from $\ell = 0$ neutron resonance spacings D_0 taken from RIPL-3 [25] assuming the following spin distribution [26]

$$g(E=S_n,I) \simeq \frac{2I+1}{2\sigma^2}\exp[-(I+1/2)^2/2\sigma^2]. \quad (4)$$

The spin-cutoff parameter σ at the neutron separation energy S_n was estimated by use of the systematics of Ref. [27]. The values of S_n, D_0, σ, and ρ are listed in Table I. Further details on the normalization procedure are described in Refs. [14,28].

Recently [16], the level densities of $^{231-233}$Th and $^{237-239}$U were reported. For the sake of completeness and to demonstrate the normalization procedure, we show in Fig. 2 the level densities for ^{232,233}Pa. The figure demonstrates how the level density is normalized to the anchor points at low and high excitation energies. It is interesting to see that only a small fraction of the levels have been observed in these isotopes, e.g., at $E \approx 1$ MeV only 10% of all levels are known. Above $E \approx 2$ MeV the level density follows the constant-temperature level density formula [26], in accordance with the findings for the other actinides. Since details on the level densities and thermodynamics have been presented recently [16], we will only focus on the γSF and the appearance of the SR in the following.

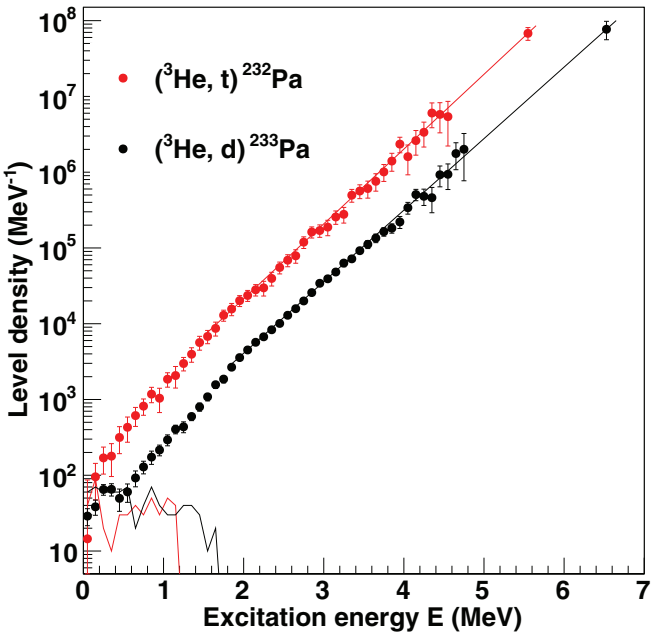

FIG. 2. (Color online) Level densities for ^{232,233}Pa. The experimental data are normalized to the level density of known discrete levels at low excitation energy E (solid lines) and the level density extracted from known neutron resonance spacings D_0 at the neutron separation energy S_n. The connection between $\rho(S_n)$ (the upper right data points) and our experimental data are made with a constant-temperature formula with $T_{\text{CT}} = 0.44$ and 0.46 MeV for ^{232,233}Pa, respectively. Note the extreme high level density for the odd-odd ^{232}Pa, which reads $\approx$ 68 million levels per MeV at $S_n = 5.55$ MeV.

III. NORMALIZATION OF THE γ-RAY STRENGTH FUNCTION

The actinides have a rapidly increasing level density with excitation energy due to a high density of single-particle orbitals. Furthermore, the presence of a low pairing gap and high-j orbitals surrounding the Fermi level produce a broad spin distribution at high excitation energy. The light-ion reactions used in this work may not populate the highest spins present in the nucleus, which in turn could influence the shape of the observed primary γ spectra P. Since the transmission coefficient $\mathcal{T}$ is assumed to be independent of spin, the observed P matrix should be fitted with the product $\mathcal{T}\rho_{\text{red}}$, where the reduced level density is extracted by a lower value of ρ at S_n. Since there are uncertainties in the total $\rho(S_n)$ through the estimate of σ and also the actual spin

distribution brought into the nuclear system by the specific reaction, the extracted slope of $\mathcal{T}$ (the α parameter) becomes rather uncertain.

The parameter B controls the scaling of the transmission coefficient $\mathcal{T}(E_\gamma)$. Here we use the average, total radiative width $\langle\Gamma_\gamma\rangle$ at S_n assuming that the γ decay is dominated by dipole transitions. For initial spin I and parity π, the width is given by [28]

$$\langle\Gamma_\gamma\rangle = \frac{1}{2\pi\rho(S_n,I,\pi)}\sum_{I_f}\int_0^{S_n} dE_\gamma B\mathcal{T}(E_\gamma) \times\rho(S_n - E_\gamma, I_f), \quad (5)$$

where the summation and integration run over all final levels with spin I_f that are accessible by $E1$ or $M1$ transitions with energy E_γ. However, the determination of B becomes also rather uncertain because the integral of Eq. (5) depends on the functions of level density $\rho(E)$ and spin-cutoff parameter $\sigma(E)$.

The above complications encountered for the actinides make the standard normalization procedure of the Oslo method rather difficult to perform. The α and B parameters have large uncertainties, and only the A parameter can be determined with a reasonable precision. Therefore, another procedure is adopted in this work where we compare the γSF with the extrapolation of known data from photonuclear reactions.

The γSF for dipole radiation can be calculated from the transmission coefficient $\mathcal{T}(E_\gamma)$ by [25]

$$f(E_\gamma) = \frac{1}{2\pi}\frac{\mathcal{T}(E_\gamma)}{E_\gamma^3}. \quad (6)$$

These data are compared with the strength function derived from the cross section σ of photonuclear reactions by [25]

$$f(E_\gamma) = \frac{1}{3\pi^2\hbar^2c^2}\frac{\sigma(E_\gamma)}{E_\gamma}. \quad (7)$$

In Fig. 3 the γSF derived from (γ, x) cross sections on ^{232}Th and ^{236,238}U by Caldwell *et al.* [29] are shown. Naturally, the data are seen to drop off when $E_\gamma < S_n$. Furthermore, we observe that the γSF does not vary much with neutron number, as seen for ^{236,238}U in panel (c). However, a comparison between ^{232}Th and ^{236}U in panel (b) reveals that the γSF increases when the proton number goes from $Z = 90$ to 92. Thus, we assume that the γSFs from ^{232}Th and ^{238}U can be applied for $^{231-233}$Th and $^{237-239}$U, respectively. For ^{232,233}Pa with $Z = 91$, we use the average values of ^{232}Th ($Z = 90$) and ^{236}U ($Z = 92$). At 7 MeV of γ energy, these two γSFs deviate with 25%. A reasonable estimate of the uncertainty in the interpolation for ^{232,233}Pa is 10%, which is much less than the uncertainty due to low statistics.

Since our data cover γ energies below S_n, we have to extrapolate the (γ, x) data to lower energies using reasonable functions. For the double-humped giant electric dipole resonance (GEDR) we fit the data with two enhanced generalized

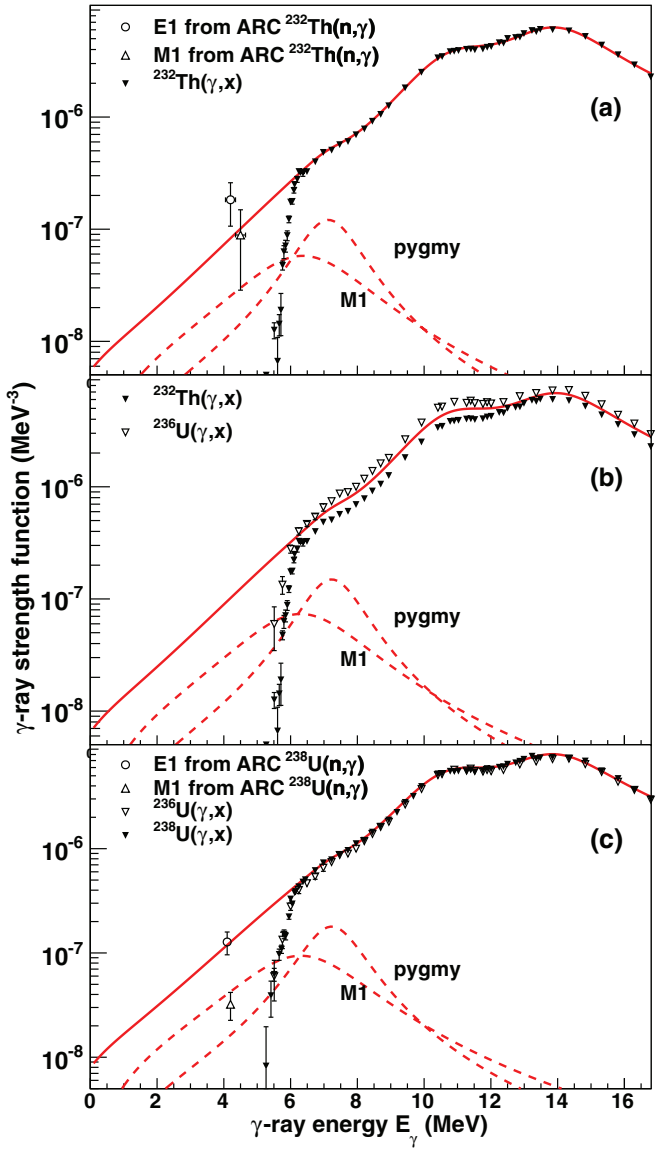

FIG. 3. (Color online) Estimation of the underlying γSF in Th (a), Pa (b), and U (c) isotopes. The red solid curve represents the strength expected without the scissors strength. The (γ, x) data are taken from Caldwell *et al.* [29] and the ARC data from Refs. [25,30]. The dashed curves are the $M1$ spin-flip resonance recommended by RIPL and an unknown pygmy resonance, which is introduced to take into account the increased strength at $E_\gamma \approx 7.3$ MeV.

Lorentzians (EGLO) as defined in RIPL [25], but with a constant temperature of the final states T_f. The (γ, x) data [29] also reveal a resonance-like bump at around 7.3 MeV (labeled pygmy in Fig. 3). This unknown resonance[2] together with the $M1$ spin-flip resonance (labeled M1 in Fig. 3) recommended by RIPL, are included in the strength as standard Lorentzian shapes. The various resonance parameters which define the solid red line shown in Fig. 3, are included in Table II. For comparison we also include in the figure the $E1$ and $M1$

[2]We will not speculate here about the origin of this resonance.

TABLE II. Resonance parameters used for γSF extrapolation.

Isotopes	$\omega_{E1,1}$ (MeV)	$\sigma_{E1,1}$ (mb)	$\Gamma_{E1,1}$ (MeV)	$\omega_{E1,2}$ (MeV)	$\sigma_{E1,2}$ (mb)	$\Gamma_{E1,2}$ (MeV)	T_f (MeV)	$\omega_{\rm pyg}$ (MeV)	$\sigma_{\rm pyg}$ (mb)	$\Gamma_{\rm pyg}$ (MeV)	ω_{M1} (MeV)	σ_{M1} (mb)	Γ_{M1} (MeV)
$^{231-233}$Th	11.5	374	4.2	14.4	840	4.2	0.2	7.2	10	2.0	6.67	4.36	4.0
^{232,233}Pa	11.5	473	4.2	14.4	900	4.2	0.2	7.3	13	2.0	6.61	5.46	4.0
$^{237-239}$U	11.4	572	4.2	14.4	1040	4.2	0.2	7.3	15	2.0	6.61	7.00	4.0

strengths derived from (n,γ) average resonance capture data (ARC) from Ref. [30].

Provided that the extrapolations in Fig. 3 (red solid lines) are reliable, we may assume that this γSF represents the "baseline" with no additional strength from other resonances. Thus, we normalize the measured γSF to this underlying background as demonstrated in Fig. 4. Here, the α parameter is adjusted to obtain the right slope of the observed γSF, and B is tuned to scale the data to the underlying background. To see the deviations from a standard normalization procedure, we also calculate the parameter values necessary to obtain the given fit to the γSF background.

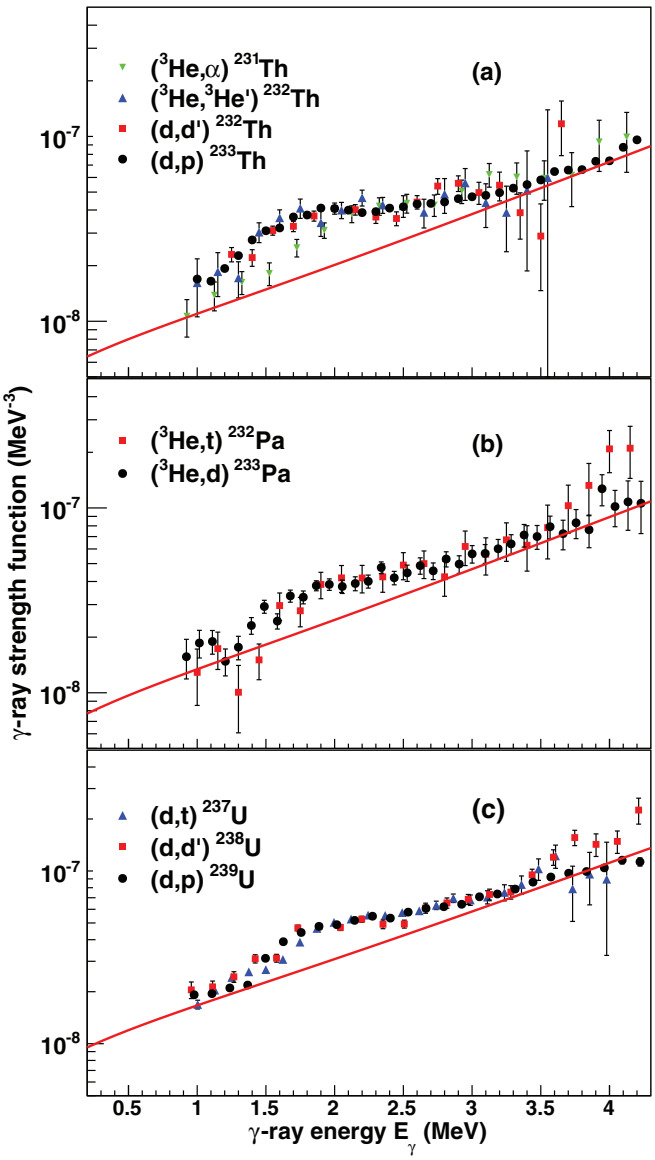

FIG. 4. (Color online) Normalization of the γ-ray strength functions with respect to the red solid curves of Fig. 3, which are assigned to the Th, Pa, and U isotopes.

The adopted values for the level density and γ width $\langle\Gamma_\gamma(S_n)\rangle$ are shown in Table I. In the case of the $(d,\ p)$ reaction it seems that about half of the spin distribution at high excitation energy is covered by the reaction. We also observe that the adopted $\langle\Gamma_\gamma(S_n)\rangle$ values deviate from the measured values. The exact reason is difficult to pin down since the normalization integral of Eq. (5) depends on how the spin-cutoff parameter, level density, and transmission coefficient vary in the whole energy region up to S_n. The observed deviations may also be due to the fact that the high excitation-energy part was in some cases poorly populated as, e.g., for ^{232}Th. Then the evaluation of Eq. (5) depends strongly on proper extrapolations of ρ and $\mathcal{T}$ in the unknown energy regions.

IV. THE SCISSORS RESONANCE

In Figs. 5–7 we have subtracted the assumed background line of Fig. 4 for the thorium, protactinium and uranium isotopes. We observe a clear overshoot of strength in the $E_\gamma = 1$–4 MeV region, which is analyzed in the following. The present SR distributions differ from the ones previously measured [17]. The main reason is that the $(\gamma,\ x)$ data of Gurevich *et al.* [31] have been replaced by the newer and more precise data of Caldwell *et al.* [29], which gives more reliable extrapolations, as shown in Fig. 3. Furthermore, the new NaI-response functions have slightly changed the SR γ-energy distributions.

Although some of the experimental γSFs are hampered by poor statistics, it appears that the additional γ strength can be decomposed into two Lorentzians. However, we should point out that large statistical errors for ^{232,233}Pa could also make these data compatible with only one broad Lorentzian.

The resonance centroid ($\omega_{{\rm SR},i}$), cross section ($\sigma_{{\rm SR},i}$), and width ($\Gamma_{{\rm SR},i}$) are listed in Table III for the lower ($i = 1$) and upper ($i = 2$) resonances. From the resonance parameters, the integrated strengths of the two components can be calculated by

$$B_{{\rm SR},i} = \frac{9\hbar c}{32\pi^2}\left(\frac{\sigma_{{\rm SR},i}\Gamma_{{\rm SR},i}}{\omega_{{\rm SR},i}}\right). \quad (8)$$

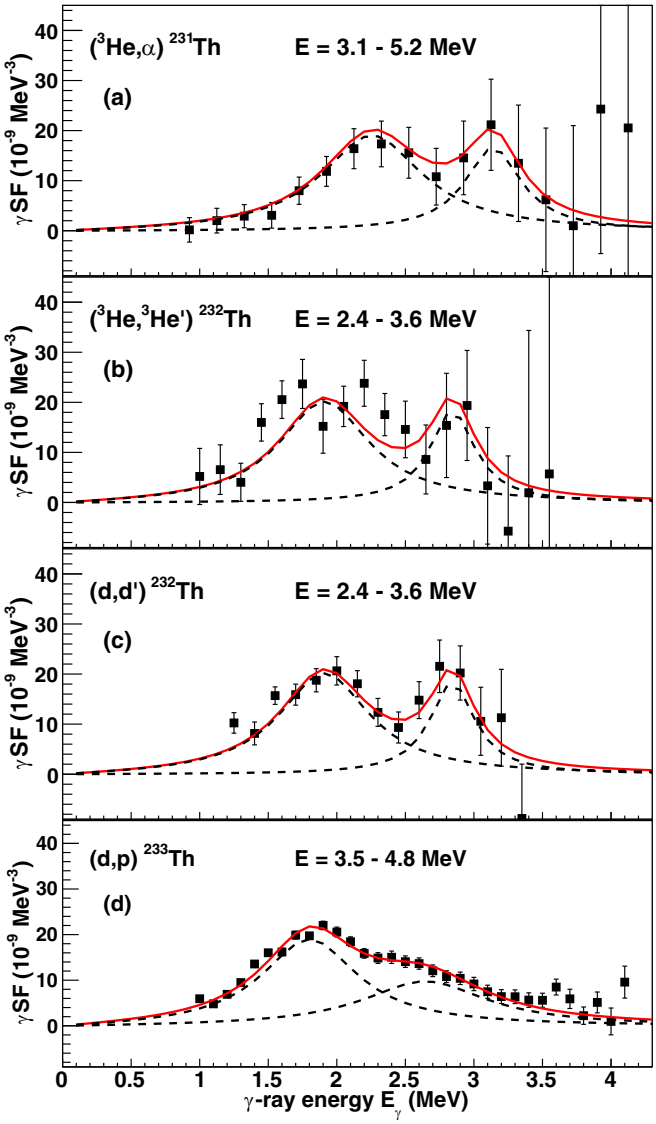

FIG. 5. (Color online) The extracted scissors resonance for $^{231–233}$Th. The various nuclei are produced with different reactions and different excitation energy regions of the primary γ matrix are utilized.

Furthermore, the total strength and the average centroid are expressed by

$$B_{\mathrm{SR}} = \sum_{i=1,2} B_{\mathrm{SR},i}, \tag{9}$$

$$\omega_{\mathrm{SR}} = \frac{\sum_{i=1,2} \omega_{\mathrm{SR},i} B_{\mathrm{SR},i}}{\sum_{i=1,2} B_{\mathrm{SR},i}}. \tag{10}$$

In Table III the upper and lower scissors strength ($B_{\mathrm{SR},i}$), together with the average centroid (ω_{SR}) and total strength (B_{SR}) are also listed.

Previous measurements for the SR built on the ground state [7–9] reveal centroids around 2.2 MeV of excitation energy, which corresponds to the first resonance in our γSF. Table III shows that, on average, the first resonance is centered around $\omega_{\mathrm{SR}} = 2.05(15)$ MeV with a strength of

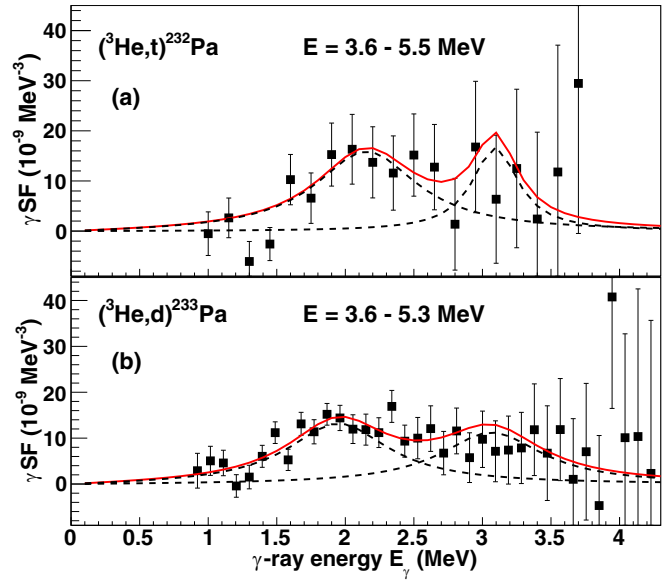

FIG. 6. (Color online) Same as Fig. 5 for $^{232–233}$Pa.

$B_{\mathrm{SR}} = 5.9(18)\mu_N^2$. Several of the mentioned studies show that levels in the $E \approx 2.2$ MeV region have spin-parity $I^\pi = 1^+$, which strongly support the interpretation as the scissors resonance. To our knowledge, the SR is the only known candidate for a soft resonance mode at these low energies.

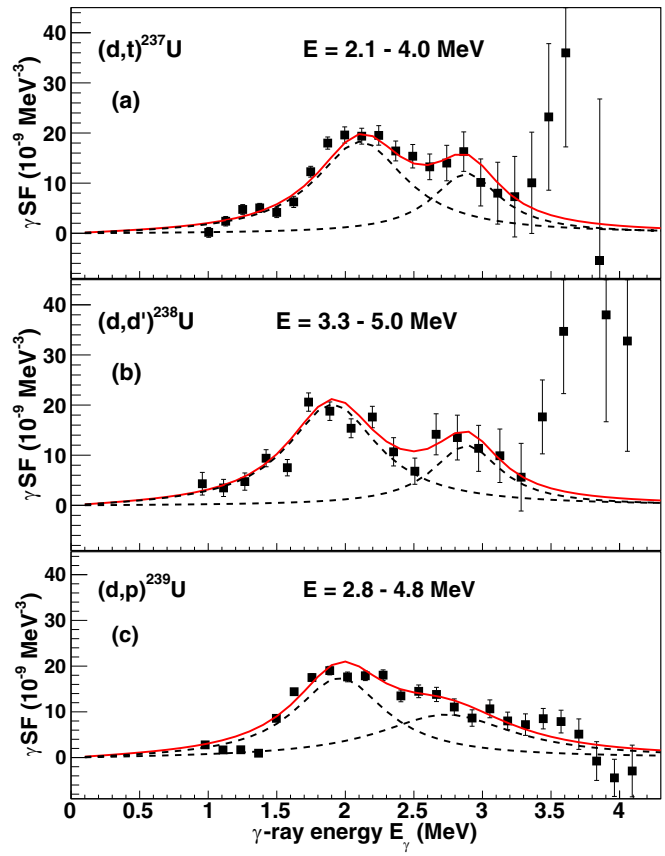

FIG. 7. (Color online) Same as Fig. 5 for $^{237–239}$U.

TABLE III. Scissors resonance parameters and the sum-rule estimates of Eqs. (19) and (20) (see text).

Nuclide	Deformation	Lower resonance				Upper resonance				Total		Sum rule	
^{A}X	δ	$\omega_{SR,1}$ (MeV)	$\sigma_{SR,1}$ (mb)	$\Gamma_{SR,1}$ (MeV)	$B_{SR,1}$ (μ_N^2)	$\omega_{SR,2}$ (MeV)	$\sigma_{SR,2}$ (mb)	$\Gamma_{SR,2}$ (MeV)	$B_{SR,2}$ (μ_N^2)	ω_{SR} (MeV)	B_{SR} (μ_N^2)	ω_{SR} (MeV)	B_{SR} (μ_N^2)
^{231}Th	0.24	2.30(15)	0.50(5)	0.90(10)	6.9(11)	3.15(15)	0.60(20)	0.50(10)	3.4(13)	2.58(15)	10.3(17)	2.0	8.6
^{232}Th	0.24	1.95(15)	0.45(10)	0.80(20)	6.5(22)	2.85(10)	0.60(20)	0.40(10)	3.0(12)	2.23(14)	9.5(26)	2.0	8.6
^{233}Th	0.24	1.85(10)	0.40(5)	0.85(10)	6.5(12)	2.70(20)	0.30(5)	1.10(20)	4.3(11)	2.19(15)	10.8(16)	2.0	8.5
^{232}Pa	0.24	2.20(20)	0.40(20)	0.90(20)	5.8(32)	3.10(30)	0.60(40)	0.40(20)	2.7(23)	2.49(24)	8.5(39)	2.0	8.7
^{233}Pa	0.25	2.00(20)	0.30(20)	0.90(30)	4.8(36)	3.10(30)	0.40(30)	0.90(30)	4.1(34)	2.51(25)	8.9(49)	2.0	9.0
^{237}U	0.26	2.15(10)	0.45(5)	0.80(10)	5.9(10)	2.90(20)	0.40(10)	0.60(15)	2.9(11)	2.40(14)	8.8(15)	2.1	9.5
^{238}U	0.27	1.95(15)	0.45(5)	0.80(10)	6.5(12)	2.90(15)	0.40(10)	0.60(15)	2.9(10)	2.24(15)	9.4(16)	2.2	9.8
^{239}U	0.25	2.00(15)	0.30(5)	0.80(10)	4.2(10)	2.80(15)	0.30(5)	1.20(20)	4.5(11)	2.41(15)	8.8(14)	2.0	9.1

Our data show a second component located on average $\Delta\omega_{SR} = 0.89(15)$ MeV higher than the lower resonance and with a strength of $3.5(16)\mu_N^2$. This component was not reported in the earlier experiments [7–9]. However, in a recent work [10] from the High-Intensity γ-ray Source (HIγS) facility at the Triangle Universities Nuclear Laboratory (TUNL) a concentration of 1^+ states was found at $E \approx 3$ MeV in ^{232}Th. These data will be compared with the present results in the next section.

V. COMPARISON WITH OTHER DATA AND MODELS

A. Other data

When comparing data and model predictions for the SR built on the ground state, it is common to quote the average excitation energy and the summed strength. For measuring of the SR built on the ground state, (γ, γ') and (e,e') reactions have been frequently used. In the past, the experimental values obtained from these reactions were rather uncertain because many weak-intensity γ (or e) lines were difficult to detect due to high backgrounds. In addition, there were also limitations on the excitation energies covered by the experiments. An indication of missing strength comes from the odd-mass deformed rare-earth nuclei, which display only half of the summed strength ($\approx 1.5\mu_N^2$) compared to their even-even neighbors ($\approx 3\mu_N^2$), which is rather surprising from a theoretical point of view. The strength is fragmented into several weak and unresolved lines in the spectra due to 5–10 times higher level density in odd-mass nuclei. An example is ^{163}Dy where new and more sensitive experiments by Nord *et al.* [32] in 2003 revealed twice the strength originally observed in 1993 by Bauske *et al.* [33].

For the actinides, the second concentration of SR states at excitation energies $E \approx 2.9$ MeV was first observed in 2011 at the HIγS facility [10]. Prior to this study, the second high-energy component was observed neither in ^{232}Th nor in ^{235,236,238}U [7–9]. The HIγS experiment on ^{232}Th not only pushed the previous [7] summed strength of $2.6(3)\mu_N^2$ up to $4.3(6)\mu_N^2$, but also revealed a two-component structure that may bring new insight to the SR mechanism.

Even though the (γ, γ') method is based on discrete population of states built on the ground state, a comparison with the present results from decay in the quasicontinuum can be made. However, one should keep in mind that these experiments represent two different systems with respect to the nuclear moment of inertia, as described in the following.

Figure 8 shows the γSF from the Oslo method [panel (a)] in ^{232}Th compared with the states measured at the HIγS facility [panel (b)] [10]. One should note that the abscissa and ordinate of these plots are different. The HIγS data are presented as discrete B_{SR} values for each state observed with γ's of

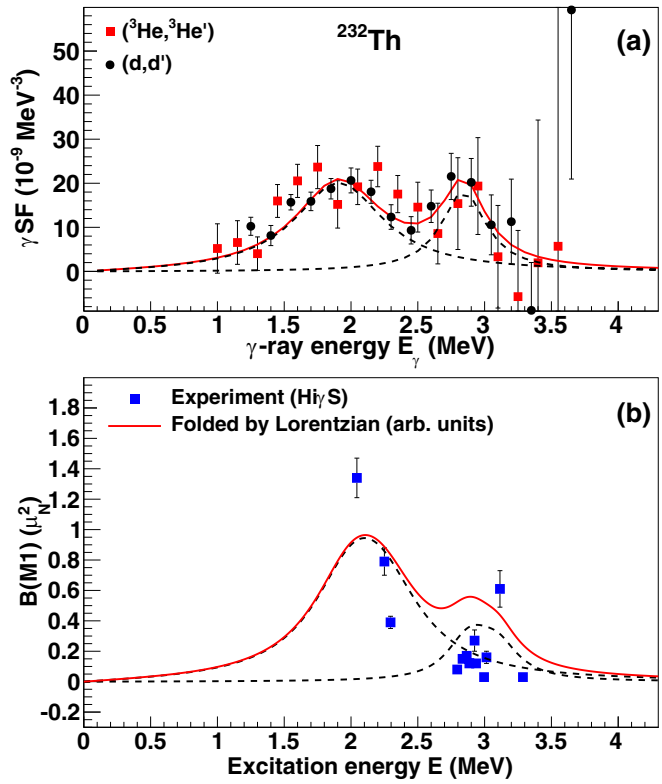

FIG. 8. (Color online) Comparison between Oslo (a) and HIγS (b) data for ^{232}Th. The HIγS data are discrete levels with measured $B(M1)$. The folded red curve of these data using Lorentzian shapes are shown in arbitrary units. The Oslo and HIγS data show some resemblance, except that the HIγS data are shifted ≈300 keV up in energy and are a factor of 2 lower in summed strength than the Oslo data (see text).

$M1$ multipolarity. According to the Brink hypothesis [13], these excitations should also be built on excited states in the continuum. In order to compare with the Oslo data, we have folded the HIγS data using two Lorentzians with widths of $\Gamma = 0.75$ and 0.35 MeV for states below and above excitation energy $E = 2.5$ MeV, respectively. These widths are chosen somewhat smaller than the widths extracted from the Oslo data in Table III since the spread in the energy positions of the 1^+ states also contributes to the width. We see from Fig. 8(b) that the two resonance peaks are located ≈ 300 keV higher than for the Oslo data. The total strength measured by the HIγS group [10] is $4.3(6)\mu_N^2$ versus the higher value of $9.5(26)\mu_N^2$ in the present study.

These results are not necessarily representing a controversy. Similar deviations have been found for the scissors strength in the deformed rare-earth region where $(\gamma,\ \gamma')$ experiments [11] typically yield strengths of $B_{\rm SR} = 3$–$4\,\mu_N^2$. Various measurements of the γ decay between levels in the quasicontinuum show significant higher SR strength. Here, the two-step cascade method and the Oslo method give integrated strengths of 6–7 μ_N^2 [34,35]. One could speculate if the lower strength in (γ, γ') experiments is due to missing states caused by low γ intensities relative to the background or because of limited excitation-energy regions. However, the deviation may also be due to the fact that the scissors strength depends on the moment of inertia that takes different values for the ground state and the levels in the quasicontinuum.

From theoretical considerations described in the next section, the strength of the SR should be proportional to the moment of inertia, which may take a lower and upper limit. In principle, for the SR built on the ground state, the ground-state moment of inertia should be applied. This quantity is easily extracted from the first rotational 2^+ state in even-even deformed nuclei by

$$\Theta_{\rm gs} = 3\hbar^2/E_{2^+}. \tag{11}$$

For the SR in the quasicontinuum, the rigid-body moment of inertia should be used:

$$\Theta_{\rm rigid} = \tfrac{2}{5} m_N r_0^2 A^{5/3}(1 + 0.31\delta), \tag{12}$$

with $r_0 = 1.15$ fm and δ is the nuclear quadrupole deformation[3] taken from [36].

In the case of ^{232}Th, we have $E_{2^+} = 0.0494$ MeV giving the lower limit $\Theta_{\rm gs}/\hbar^2 = 60.7$ MeV^{-1}, while the rigid value becomes $\Theta_{\rm rigid}/\hbar^2 = 120.8$ MeV^{-1}, which represents the upper limit. It is interesting that the ratio $\Theta_{\rm rigid}/\Theta_{\rm gs} = 2.0$ is in agreement with the ratio $\sum B(M1)_{\rm Oslo}/\sum B(M1)_{\rm HI\gamma S} = 2.2(7)$ for ^{232}Th. A similar scaling is valid also for the well deformed rare-earth region. These observations may call for a consistent model that is capable of describing the SR states built on the ground state as well as the SR distribution in the quasicontinuum.

[3]In this work, we use the quadrupole deformation parameter δ, which relates to the deformation parameters ϵ_2 and β_2; to lowest order $\delta \approx \epsilon_2 \approx \beta_2\sqrt{45/16\pi}$.

B. Models

Numerous SR models have been launched to explain the results of the $(\gamma,\ \gamma')$ and (e,e') reactions [11]. The predictions for deformed rare-earth nuclei were often guided by the measured values found at the time when the models were published. Quasiparticle random phase approximation (QRPA) models are rather popular, although these also have some freedom for tuning the results to experimental data. A common definition [37] of an SR state is when the orbit-to-spin ratio is $|M_l/M_s|^2 \gg 1$. In the work of Kuliev *et al.* [12], QRPA calculations were performed for the $E = 2$–4 MeV excitation region. Their calculations for ^{232}Th and ^{236,238}U give typical strengths of $\sum B = 5$–$6\,\mu_N^2$ at the average excitations energy of $E = 2.6$ MeV. With a moment of inertia ratio of $\Theta_{\rm rigid}/\Theta_{\rm gs} \approx 2.0$ these predictions are in agreement with the present findings.

It is interesting to investigate the most important single-particle orbitals responsible for the SR in the QRPA calculations [12]. The various SR states are composed of several pairs of Nilsson orbitals, having $\Delta\Omega = 1$. The most pronounced pairs of the strongest SR states at low excitation in ^{232}Th and ^{238}U are $\frac{1}{2}^-[530]_p \otimes \frac{3}{2}^-[521]_p$ and $\frac{5}{2}^+[642]_p \otimes \frac{7}{2}^+[633]_p$, respectively. The strongest and higher-lying SR states of ^{232}Th, are calculated to have excitation energies of 2.998 and 3.134 MeV. Their wave-functions are dominated by [38] the $\frac{3}{2}^+[402]_p \otimes \frac{5}{2}^+[402]_p$ and $\frac{1}{2}^+[541]_p \otimes \frac{1}{2}^+[530]_p$ configurations, respectively. The mechanism behind the splitting of the strength into two energy regions is not clear, other than the distance of the Nilsson orbitals to the Fermi surface has some relevance. The strong admixture of many two-quasiparticle orbitals in the SR states indicates that these excitations are rooted in collective motion.

In this work we have chosen the sum-rule approach [39], which is a rather fundamental way of predicting both $\omega_{\rm SR}$ and $B_{\rm SR}$. The drawback is that only these two gross properties are given. This approach requires that the strength be located at one specific excitation energy, and is not able to explain why the SR distribution splits into two components.

We follow the description of Enders *et al.* [40] with the exception that the ground-state moment of inertia will be replaced by the rigid-body moment of inertia. The inversely and linearly energy-weighted sum rules are given by

$$S_{+1} = \frac{3}{8\pi}\Theta_{\rm rigid}\delta^2\omega_D^2(g_p - g_n)^2\left[\mu_N^2{\rm MeV}\right], \tag{13}$$

$$S_{-1} = \frac{3}{16\pi}\Theta_{\rm IV}(g_p - g_n)^2\left[\mu_N^2{\rm MeV}^{-1}\right]. \tag{14}$$

For the g factors[4] we use the common expression $g_p - g_n \approx 2Z/A$, which rests on the assumption that the neutron and rotational gyromagnetic factors are $g_n \approx 0$ and $g_R \approx (g_p + g_n)/2 \approx Z/A$, respectively [41]. Since the SR is measured in the quasicontinuum, the isovector moment of inertia $\Theta_{\rm IV}$ is taken as the rigid-body moment of inertia $\Theta_{\rm rigid}$ as discussed above.

[4]Bare gyromagnetic factors are $g_p = 1$ and $g_n = 0$.

According to Enders *et al.* [40] the $K = 1$ component of the isovector giant quadrupole resonance (IVGQR) will dominate S_{+1} and has to be removed using a reduction factor

$$\xi = \frac{\omega_Q^2}{\omega_Q^2 + 2\omega_D^2} \tag{15}$$

that depends on the energy centroids of the isovector giant dipole (IVGDR) and isoscalar giant quadrupole (ISGQR) resonances:

$$\omega_D \approx (31.2A^{-1/3} + 20.6A^{-1/6})(1 - 0.61\delta)\ \text{MeV}, \tag{16}$$

$$\omega_Q \approx 64.7A^{-1/3}(1 - 0.3\delta)\ \text{MeV}. \tag{17}$$

In the mass region investigated here, ξ is rather independent on A (and δ) and takes the value $\xi \approx 0.27$. The adequate expression of S_{+1} for the low-lying scissors mode then reads

$$S_{+1} = \frac{3}{2\pi}\Theta_{\text{rigid}}\delta^2\omega_D^2 g_{\text{IS}}^2\xi, \tag{18}$$

where $g_{\text{IS}} = \frac{1}{2}(g_p + g_n) \approx Z/A$.

The two sum rules can now be utilized to extract the SR centroid and strength:

$$\begin{aligned}\omega_{\text{SR}} &= \sqrt{S_{+1}/S_{-1}} \\ &= \delta\omega_D\sqrt{2\xi},\end{aligned} \tag{19}$$

$$\begin{aligned}B_{\text{SR}} &= \sqrt{S_{+1}S_{-1}} \\ &= \frac{3}{4\pi}\left(\frac{Z}{A}\right)^2\Theta_{\text{rigid}}\delta\omega_D\sqrt{2\xi}.\end{aligned} \tag{20}$$

It is interesting to note that S_{-1} does not depend on ξ. Thus, if the experimental $\omega_{\text{SR}}^{\text{exp}}$ is known, a less rigorous relation for the strength is

$$\begin{aligned}B_{\text{SR}} &= \omega_{\text{SR}}^{\text{exp}}S_{-1} \\ &= \omega_{\text{SR}}^{\text{exp}}\frac{3}{4\pi}\left(\frac{Z}{A}\right)^2\Theta_{\text{rigid}},\end{aligned} \tag{21}$$

which replaces the centroid from the sum rule with the experimental value. However, this was not necessary in the present work since both the centroid and strength are well described by the sum rules.

The total SR strength and weighted centroid for the eight nuclei of Figs. 5–7 are summarized in Table III. The two last columns of Table III show the predicted sum-rule estimates. Both the ω_{SR} and B_{SR} values are in good agreement with our measurements. Although S_{-1} depends very weakly on δ, the ω_{SR} follows a δ dependence; see Eq. (19). However, since $B_{\text{SR}} = \omega_{\text{SR}}S_{-1}$ the strength follows $\approx \delta$, contrary to the strong δ^2 dependence for SR states built on the ground state [42,43]. Unfortunately, our data do not allow us to conclude any systematic behavior regarding A or δ; all eight nuclei display the same resonance parameters within the experimental errors.

In Fig. 9 we have plotted the sum-rule estimates for ^{232}Th and compared to the experimental values. With the assumption of a rigid-body moment of inertia in the quasicontinuum, the Oslo data are very well reproduced at a deformation of $\delta = 0.24$. For illustration, it is interesting to show the sum-rule estimates for different deformations, still assuming the ^{232}Th system. The sum rule predicts that the centroid as well as the strength will decrease linearly with δ as one approaches more spherical nuclei. For the HIγS data the strength and centroid are overestimated by the sum-rule approach using ground-state moment of inertia. In this case, one cannot calculate the δ dependence directly from the sum rule as the E_{2^+} energy is unknown for deformations differing from the deformation of ^{232}Th with $\delta \approx 0.24$. However, it is well known that the average centroid is approximately constant and the strength follows a $\approx\delta^2$ rule [40]. These dependencies are indicated as dashed blue lines in Fig. 9. It would be very interesting to follow the SR in the quasicontinuum to lower deformations to see if the strength and centroid decrease as expected.

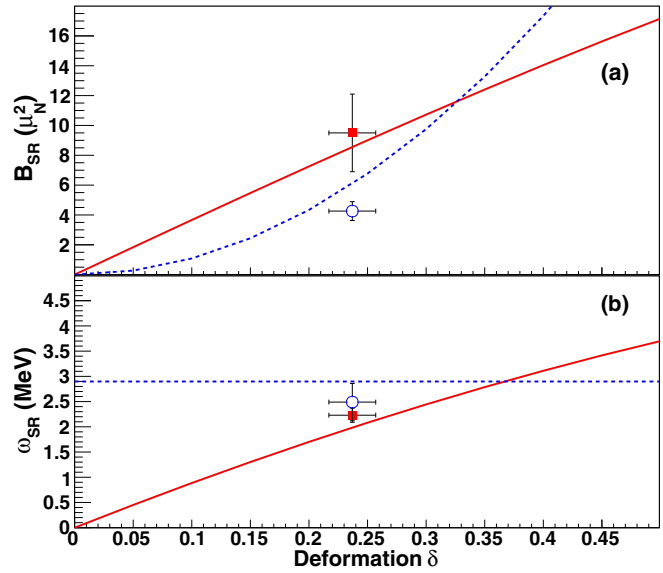

FIG. 9. (Color online) Comparison between observed SRs for ^{232}Th from Oslo and HIγS. The data are compared with sum-rule estimates using Θ_{rigid} and Θ_{gs} for the two experiments, respectively. The deformation dependence for SR built on the ground state is assumed to be constant for ω and follows a δ^2 rule for $\sum B(M1)$.

Over the last 30 years many theoretical works have been published for the SR built on the ground state [11]. However, the centroid and strength of the SR in the quasicontinuum is the quantity that directly relates to the reaction rates in, e.g., astrophysical environments. For example, for the r process, which involves nuclei with extreme N/Z ratios, the decrease in neutron-separation energy with neutron number is expected to give an increasing impact from the SR on the reaction rates. The SR represents also an important ingredient for the simulations of fuel cycles for fast nuclear-power reactors. Sensitivity and uncertainty studies [44,45] for reactors included in the Generation IV (Gen IV) initiative and accelerator driven systems (ADS) show that the cross sections involved must be known with high precision. Thus, there is a great need for new theoretical and experimental investigations of the summed SR strength, its dependence on the deformation, and the origin of the two-component structure seen here in the quasicontinuum of the actinides.

VI. CONCLUSIONS

The level densities of $^{232–233}$Pa and the γSFs of $^{231–233}$Th, ^{232,233}Pa and $^{237–239}$U have been determined using the Oslo method. The level densities show a constant-temperature behavior as recently reported for $^{231–233}$Th and $^{237–239}$U.

All the eight actinides investigated show an excess in the γSFs in the $E_\gamma = 1$–4 MeV region, which is interpreted as the scissors resonance in the quasicontinuum. The underlying strength has been subtracted by extrapolating the assumed strength from the tails of other resonances; the double humped GEDR, the spin-flip GMDR and an unknown pygmy resonance.

The sum rule applied to the quasi-continuum gives a satisfactory description of the SR for all isotopes studied. The approach predicts that ω_{SR} and B_{SR} are proportional to the deformation parameter δ. This is in contrast with the δ^2 behavior of the SR built on the ground state. Furthermore, the SR shows a splitting into two components, which is in accordance with data from the HIγS facility. However, there are currently no firm theoretical explanations of the two-component structure seen in the present study. Theoretical and experimental studies of the SR in the quasicontinuum are called for to obtain reliable reaction rate predictions used in nuclear-astrophysics and reactor applications.

ACKNOWLEDGMENTS

We would like to thank J. C. Müller, E. A. Olsen, A. Semchenkov and J. Wikne at the Oslo Cyclotron Laboratory for providing the stable and high-quality deuterium and ^{3}He beams during the experiment, the Lawrence Livermore National Laboratory for providing the ^{232}Th target and the GSI Target Laboratory for the production of the ^{238}U target. We thank A.A. Kuliev, E. Guliyev and F. Ertugral for sharing details of their QRPA calculations. This work was supported by the Research Council of Norway (NFR), the French national research programme GEDEPEON, the U.S. Department of Energy under Contract No. DE-AC52-07NA27344, the National Research Foundation of South Africa, the European Commission within the 7th Framework Programme through Fission-2010-ERINDA (Project No. 269499) and by the European Atomic Energy Communitys 7th Framework Programme under Grant Agreement No. FP7-249671 (ANDES).

[1] M. Arnould, S. Goriely, and K. Takahashi, Phys. Rep. **450**, 97 (2007).
[2] F. Käppeler *et al.*, Rev. Mod. Phys. **83**, 157 (2011).
[3] M. B. Chadwick *et al.*, Nucl. Data Sheets **112**, 2887 (2011).
[4] N. Lo Iudice and F. Palumbo, Phys. Rev. Lett. **41**, 1532 (1978).
[5] Y. S. Chen and G. A. Leander, Phys. Rev. C **26**, 2607 (1982).
[6] M. Guttormsen, J. Rekstad, A. Henriquez, F. Ingebretsen, and T. F. Thorsteinsen, Phys. Rev. Lett. **52**, 102 (1984).
[7] R. D. Heil, H. H. Pitz, U. E. P. Berg, U. Kneissl, K. D. Hummel, G. Kilgus, D. Bohle, A. Richter, C. Wesselborg, and P. von Brentano, Nucl. Phys. A **476**, 39 (1988).
[8] J. Margraf, A. Degener, H. Friedrichs, R. D. Heil, A. Jung, U. Kneissl, S. Lindenstruth, H. H. Pitz, H. Schacht, U. Seemann, R. Stock, C. Wesselborg, P. von Brentano, and A. Zilges, Phys. Rev. C **42**, 771 (1990).
[9] O. Yevetska, J. Enders, M. Fritzsche, P. von Neumann-Cosel, S. Oberstedt, A. Richter, C. Romig, D. Savran, and K. Sonnabend, Phys. Rev. C **81**, 044309 (2010).
[10] A. S. Adekola, C. T. Angell, S. L. Hammond, A. Hill, C. R. Howell, H. J. Karwowski, J. H. Kelley, and E. Kwan, Phys. Rev. C **83**, 034615 (2011).
[11] K. Heyde, P. von Neumann-Cosel, and A. Richter, Rev. Mod. Phys. **82**, 2365 (2010), and references therein.
[12] A. A. Kuliev, E. Guliyev, F. Ertugral, and S. Özkan, Eur. Phys. J. A **43**, 313 (2010).
[13] D. M. Brink, Ph.D. thesis, Oxford University, 1955 (unpublished).
[14] A. Schiller *et al.*, Nucl. Instrum. Methods Phys. Res., Sect. A **447**, 498 (2000).
[15] A. C. Larsen *et al.*, Phys. Rev. C **83**, 034315 (2011).
[16] M. Guttormsen *et al.*, Phys. Rev. C **88**, 024307 (2013).
[17] M. Guttormsen, L. A. Bernstein, A. Bürger, A. Görgen, F. Gunsing, T. W. Hagen, A. C. Larsen, T. Renstrøm, S. Siem, M. Wiedeking, and J. N. Wilson, Phys. Rev. Lett. **109**, 162503 (2012).
[18] M. Guttormsen, A. Bürger, T. E. Hansen, and N. Lietaer, Nucl. Instrum. Methods Phys. Res., Sect. A **648**, 168 (2011).
[19] M. Guttormsen *et al.*, Phys. Scr., **T32**, 54 (1990).
[20] M. Guttormsen, T. S. Tveter, L. Bergholt, F. Ingebretsen, and J. Rekstad, Nucl. Instrum. Methods Phys. Res., Sect. A **374**, 371 (1996).
[21] M. Guttormsen, T. Ramsøy, and J. Rekstad, Nucl. Instrum. Methods Phys. Res., Sect. A **255**, 518 (1987).
[22] P. A. M. Dirac, Proc. R. Soc. London A **114**, 243 (1927).
[23] E. Fermi, *Nuclear Physics* (University of Chicago Press, Chicago, 1950).
[24] Data extracted using the NNDC On-Line Data Service from the ENSDF database.
[25] R. Capote *et al.*, Reference Input Library, RIPL-2 and RIPL-3, available online at http://www-nds.iaea.org/RIPL-3/.
[26] A. Gilbert and A. G. W. Cameron, Can. J. Phys. **43**, 1446 (1965).
[27] T. von Egidy and D. Bucurescu, Phys. Rev. C **72**, 044311 (2005); **73**, 049901(E) (2006).
[28] A. Voinov, M. Guttormsen, E. Melby, J. Rekstad, A. Schiller, and S. Siem, Phys. Rev. C **63**, 044313 (2001).
[29] J. T. Caldwell, E. J. Dowdy, B. L. Berman, R. A. Alvarez, and P. Meyer, Phys. Rev. C **21**, 1215 (1980); available at http://cdfe.sinp.msu.ru/services/unifsys/index.html.
[30] J. Kopecky and M. Uhl, Phys. Rev. C **41**, 1941 (1990).
[31] G. M. Gurevich *et al.*, Zh. Eksp. Teor. Fiz., Pisma Redakt. **20**, 741 (1974).
[32] A. Nord *et al.*, Phys. Rev. C **67**, 034307 (2003).
[33] I. Bauske *et al.*, Phys. Rev. Lett. **71**, 975 (1993).
[34] M. Krtička *et al.*, Phys. Rev. Lett. **92**, 172501 (2004).
[35] A. Schiller *et al.*, Phys. Lett. B **633**, 225 (2006).
[36] S. Goriely, N. Chamel, and J. M. Pearson, Phys. Rev. Lett. **102**, 152503 (2009).

[37] R. Nojarov *et al*., Nucl. Phys. A **563**, 349 (1993).
[38] A. A. Kuliev, E. Guliyev, and F. Ertugral (private communication).
[39] E. Lipparini and S. Stringari, Phys. Rep. **175**, 103 (1989).
[40] J. Enders, P. von Neumann-Cosel, C. Rangacharyulu, and A. Richter, Phys. Rev. C **71**, 014306 (2005).
[41] A. Bohr and B. Mottelson, *Nuclear Structure*, Vol. 2 (Benjamin, New York, 1975).
[42] W. Ziegler, C. Rangacharyulu, A. Richter, and C. Spieler, Phys. Rev. Lett. **65**, 2515 (1990).
[43] P. von Neumann-Cosel, J. N. Ginocchio, H. Bauer, and A. Richter, Phys. Rev. Lett. **75**, 4178 (1995).
[44] G. Aliberti, G. Palmiotti, M. Salvatores, T. K. Kim, T. A. Taiwo, M. Anitescu, I. Kodeli, E. Sartori, J. C. Bosq, and J. Tommasi, Ann. Nucl. Energy **33**, 700 (2006).
[45] G. Aliberti, G. Palmiotti, M. Salvatores, and C. G. Stenberg, Nucl. Sci. Eng. **146**, 13 (2004).